Journal of Energy Storage 40 (2021) 102782

Contents lists available at ScienceDirect

Journal of Energy Storage

journal homepage: www.elsevier.com/locate/est

Improving the performance of trays solar still using wick corrugated absorber, nano-enhanced phase change material and photovoltaics-powered heaters

A.S. Abdullah [a,d,*], Z.M. Omara [b], F.A. Essa [b], M.M. Younes [b], S. Shanmugan [c], Mohamed Abdelgaied [d], M.I. Amro [d], A.E. Kabeel [d,e], W.M. Farouk [f]

[b] Mechanical Engineering Department, College of Engineering, Prince Sattam bin Abdulaziz University, KSA.
[a] Mechanical Engineering Department, Faculty of Engineering, Kafrelsheikh University, Kafrelsheikh, Egypt.
[c] Research Centre for Solar Energy, Department of Physics, Koneru Lakshmaiah Education Foundation, Green Fields, Guntur District, Vaddeswaram, Andhra Pradesh 522502, India.
[d] Mechanical Power Engineering Department, Faculty of Engineering, Tanta University, Tanta, Egypt.
[e] Faculty of Engineering, Delta University for Science and Technology, Mansoura Gamasa, Egypt.
[f] Mechanical Engineering Department, Faculty of Engineering, Benha University, Benha, Egypt

ARTICLE INFO

Keywords:
Trays solar still
Wick
Phase change material
Corrugated
Nanoparticle, PV module

ABSTRACT

In this study, an experimental work has been conducted to augment the performance of trays solar still. The absorber surface area and rate of heat transfer between the absorber and the saline water have been increased. Hence, the trays solar stills with flat and corrugated absorber configurations were investigated. Three solar stills have been fabricated and tested. The tested solar stills are flat trays solar still (FTSS), corrugated trays solar still (CTSS), and conventional solar still (CSS). Wick material has been used to cover the corrugated where the wick feed water flows very slowly through the porous material upward. For further improvement of trays solar still performance, phase change material (PCM) mixed with CuO nanoparticles has been used to test the CTSS. Also, three electric heaters have been used to heat the basin water. The heaters derived their energy directly from a PV module. The PV module was installed directly beside the back side of the solar still thereby utilizing the same solar still space. Experimental results obtained showed that, the total freshwater yield of the CTSS was improved by 150 and 122% when using electric heaters and the and PCM with CuO nanoparticles, respectively, over that of the CSS. In addition, the total water production of the CTSS was improved by 180% when using corrugated absorber, PCM mixed with CuO nanoparticles and electrical heaters in comparison to the CSS.

1. Introduction

Although water is an essential fluid that supports human lives on Earth, about 800 million people are having problem of drinkable water. Consequently, scientists presented the various methods of extracting potable water from salt water as the only means of escape from the drinking water problem facing the world. For instance, we find the reverse osmosis (RO) [1], humidification dehumidification (HDH) [2-4], vapor compression (VC) [5], multi-stage flash (MSF) [6], multi-effect boiling (MEB) [7], solar still (SS) [8,9], etc, as proposed common techniques for water distillation.

The solar distillers are small units of desalination that can be used to achieve the freshwater needs of small families because they have low productivities. Several research works have been conducted to maximize the productivity of SS systems, by minimizing the basin water depth [10-11], increasing the feed water temperature by employing solar water heaters [12-14], integrating reflectors to enlarge the incident solar energy to the SS [15-16]. In addition, the scholars tried to make modifications on the conventional solar distiller to increase its fresh water distillate [17-19]. Most of these modifications included the wick, corrugated and finned SS [20-23], stepped solar distiller [24-26], adding rotating elements to maximize the evaporation area as well as the exposed area to solar energy and to break the basin water surface tension, blades solar still [27-29], rotating wick SS [30,31], tubular drum SS [32], disc SS [33] and rotating-drum SS [34-36]. Thermophysical properties of Nanofluids such as density, convective heat transfer

* Corresponding author.
E-mail address: asbekhatro@yahoo.com (A.S. Abdullah).

https://doi.org/10.1016/j.est.2021.102782
Received 15 January 2021; Received in revised form 19 April 2021; Accepted 27 May 2021

coefficient, thermal conductivity has been investigated by several studies, exploring different materials and particle sizes [37-38].

When salinity increases in basin water, the vapor pressure reduces at water surface, which leads to slow down the evaporation process, Al-Shammiri [39]. As a result, with an increase in salinity, the water productivity decreases. Badran et al. [40] reported that when the salinity of water was reduced from 35000 ppm to 6000 ppm, the productivity increased from 2.5 to 2.8 L/day. Akash et al. [41] reported the adverse effect of basin water salt concentration on solar still fresh water production. Kalbasi and Esfahani [42] conducted an experimental study and reported that increasing the basin water salinity from 0 to 3.5% reduced the fresh water production by 20%. The effect of salt concentration on the solar still productivity was studied for saline water at a TDS of 2000 ppm, 5000 ppm and 8000 ppm with the basin water amount of 3.5 L, Asiful et al. [43]. The results revealed that the average water production was 508 mL, 488 mL and 471 mL for basin water TDS values of 2000, 5000 and 8000 ppm, respectively. With increasing the TDS from 2000 to 8000 ppm, the water production was declined by 7.28%.

It is well known that decreasing the heat losses from the glass cover, basin liner and walls increases the rate of condensation of the water vapor in the distiller. Ranjan et al. [44] reported the loss of 61.6% of the incidence solar energy on the CSS distiller, thereby utilizing only 38.4% of the solar incidence energy for the water evaporation. Similarly, the distiller walls and basin liner loses about 25.7% of the incidence solar energy. The performance of the solar still was significantly affected by these losses.

Among the methods used for reducing the losses and improving the performance of the solar still distillers is a new design called trays solar still. The performance of a novel SS namely trays solar still (TSS) has been experimentally and theoretically investigated by Abdullah et al. [45,46]. The TSS design resulted from modifying the CSS by adding trays internally as well as adding internal and external mirrors at the top and bottom. The addition of mirrors and trays to the internal sides of the SS decreases the side walls temperature and accordingly reduces the rate of heat loss to the environment. The results showed that the TSS employing both internal and external mirrors showed 95% increase in the productivity than that of CSS. In a sequential work, Abdullah et al. [47], investigated the influence of painting the trays solar still surfaces with the mixture of black paint and copper oxide (CuO) nanoparticles for the purpose of enhancing the convective heat transfer coefficient between the water and the basin surfaces. In addition, the performance of trays solar distiller with phase change material (PCM) (paraffin wax mixed with CuO nanoparticles) was experimentally investigated. The obtained results showed that, the total freshwater yield improved by about 108% compared to the CSS when using internal mirrors, PCM with CuO nanoparticles and nano coating.

Phase change materials (PCMs) can be used to reduce the rate of heat losses, during the peak solar radiation these materials can store energy and release the stored energy when the sun is not available during the night. In the absence of the solar radiation, the PCM is the heat source for the water evaporation in the basin [48,49]. Also, the phase change materials significantly improves the productivity [50]. Furthermore, mixing CuO nanoparticles with paraffin wax showed superior performance as a PCM [51]. The effects of using various nanoparticles (copper oxide, aluminum oxide and titanium oxide) on the solar still performance was evaluated by Sahota and Tiwari [52]. The aluminum oxide provided maximum solar still thermal and exergy efficiencies of 50.34% and 14.10%, respectively.

From the previous review, it can be deduced that solar still distillation methods need considerable development to increase system productivity. The aim of this study is to increase the evaporation area for trays solar stills by using new absorber configuration (corrugated) instead of flat absorber. So, the evaporation area and absorber area for trays solar still have been increased. The corrugated base is covered with wick material, the wick feed water flows very slowly through porous material upward. In addition the wick capillarity helped in exposing small amount of water to solar radiation in the evaporation surface without need to heat bulk water as in the CSS case. For further increase in trays SS performance, the caves beneath the corrugated absorber have been filled with phase change material and nanoparticles. Moreover, we used electric heaters to raise the basin water temperature of corrugated trays solar still (CTSS), which affects positively the evaporation of the investigated trays solar still. These electric heaters were operated by the energy coming from a photovoltaic panel (PV) system. The wick was involved in all CTSS cases.

2. Experimental setup and procedures

The design of this solar distillation system employs the use of locally available materials, as shown in Fig. 1. Three solar stills were constructed; CSS, FTSS and CTSS in order to compare their performance and evaluate the efficacy of adding trays to the SS sides, corrugated absorber and PCM with CuO. The dimensions of CSS, FTSS and CTSS have been illustrated in Fig. 2. The CSS is made by bending 1.5 mm thick galvanized steel sheet of 1m × 1m area. The length of high-side, low-side and basin width were 0.4 m, 0.15 m and 0.5 m, respectively. The two sides were welded to the bent galvanized sheet, forming the CSS having a basin area of 0.5 m^2, as illustrated in Fig. 2. Glass cover of 3mm thickness was used as condensation surface for all solar stills with inclination angle of 24^o which is the latitude of Al Kharj, KSA. The solar stills have been painted black (matt dark black paint) from inside to augment the SS absorptivity of solar energy. Additionally, fiberglass has been used as thermal insulating material for solar stills bottom and side areas.

FTSS has also been constructed in similar manner with the same dimensions as CSS with two modifications. Firstly, addition of trays to three internal side walls of the solar still as shown in Fig. 2. Secondly, using internal mirrors on the areas between the side trays, as shown in Fig. 2. Similarly, the corrugated solar still shown in Fig. 2 has the same construction and dimensions as the FTSS except in the shape of the still base which has corrugated form with a height of 40 mm instead of flat base. All the bends angles were 90°, and the space between any two tops was kept at 80 mm. The corrugated still base has 12 tops and 19 bottoms of corrugated form. The corrugated base is covered with wick material, the wick feed water flows very slowly through a porous to upward. The performance of CTSS has been tested with paraffin wax and CuO nanoparticles as thermal storage material. The cavity under the corrugated absorbers have been filled with paraffin wax as shown in Fig. 2.

Nanoparticles (CuO) have been added to the paraffin wax at 2.5% mass fraction (25 g CuO + 975 g paraffin wax). The properties of the paraffin wax and paraffin wax with 2.5 wt% nanoparticles are presented in Table 1 the properties of the CuO nanoparticles is presented in Table 2. The variation of thermal conductivity of PCM with nanoparticles at different nanoparticles concentration is indicated in Table 3. It is evident from the table that the thermal conductivity of the wax-nano mixture increases by increasing the concentration of nanoparticles until it reaches a ratio of 2.5wt%, and then approximately the conductivity stability occurs with the increase in the concentration of nanoparticles. So, in this work, a concentration ratio of 2.5wt% was chosen. Moreover, we wanted to investigate the influence of heating the basin water using three electric heaters with a power of 30 W each. The heaters were immersed into the basin water of the CTSS still to heat the water of the still. These electric heaters were operated by the energy coming from a photovoltaic panel (PV) system with a power of 120 W.

Under the outdoor climate of Prince Sattam bin Abdulaziz University, Al Kharj, KSA, the experimental measurements have been recorded during May and June 2020. To measure the different variables influencing the SS performance, suitable measuring apparatus have been used. A data logging solarimeter (0 – 5000 W/m^2) has been used to measure the solar radiation intensity. Besides, for measuring the temperatures of absorber, water and glass cover at different points, a G4L-CUEA modular programmable logic control (MPLC) connected to K-type thermocouples has been used. Additionally, the distillate

Fig. 1. Pictorial view of tested solar stills.

productivity is collected and evaluated hourly by a calibrated flasks of 2000 ml capacity. Moreover, the air velocity has been measured by using an Anemometer of 0.4 – 30 m/s measuring range. The Multimeter has been used to measure the output of PV panel. The experimentations were carried out at 2 cm basin water depth for basin and trays. The basin water quantity is kept at the same level (approximately) by feeding the stills manually every half an hour with an amount of saline water equal to the distillate.

3. Experimental error analysis

The uncertainty in the measured data has been estimated using Holman method [53]. Assume that a group of measurements have been carried out to estimate "n" number of experimental parameters. Based on these measurements the desired experimental result 'R' can be obtained.

Thus;

$$R= R(X_1, X_2, X_3, ..., X_n) \quad \text{..... (1)}$$

Let the uncertainty in the result is W_R and W_1, W_2, W_3, ..., W_n are the uncertainties in the independent variables. So, W_R can be calculated the following equation (Holman [53]):

$$W_R = \left[\left(\frac{\partial R}{\partial X_1}W_1\right)^2 + \left(\frac{\partial R}{\partial X_2}W_2\right)^2 + \ldots + \left(\frac{\partial R}{\partial X_n}W_n\right)^2\right]^{\frac{1}{2}} \quad (2)$$

If the result and measured parameters have a known relationship and the uncertainty associated to each measurement is also known, then W_R can be assessed using Equation (2). Table 4 shows the uncertainties of the experimental measuring apparatuses.

The hourly distillate, $m = f(h)$,

Where, h is the height of water level in the calibrated flask. From Equation (2), the total uncertainty associated with the hourly freshwater production can be reduced to:

$$W_m = \left[\left(\frac{\partial m}{\partial h}W_h\right)^2\right]^{\frac{1}{2}} \quad (3)$$

The uncertainties associated with the calculations for thermal efficiency (η). The equation of η is, $\eta_{th} = \frac{\dot{m}\times h_{fg}}{A\times I(t)}$

Since A is constant and assuming h_{fg} is constant then,

$$\eta_{th} = f(\dot{m},\ I(t)) \quad (4)$$

From Equation (2), the total uncertainty of η can be derived as,

$$W_{\eta_{th}} = \left[\left(\frac{\partial \eta_{th}}{\partial m}W_m\right)^2 + \left(\frac{\partial \eta_{th}}{\partial I_R}W_{I(t)}\right)^2\right]^{\frac{1}{2}} \quad (5)$$

The output power of PV panel, $P = f(V, I)$

Where, V is output voltage and I is the output current. The uncertainties associated with the calculations for output power of PV panel (P) can be derived as,

$$W_{\eta_{th}} = \left[\left(\frac{\partial \eta_{th}}{\partial m}W_m\right)^2 + \left(\frac{\partial \eta_{th}}{\partial I_R}W_{I(t)}\right)^2\right]^{\frac{1}{2}} \quad (6)$$

Accordingly, the errors associated with the calculated quantity of daily yield, thermal efficiency η and output power of PV panel are about ± 1.2%, ± 3% and 2.4%, respectively.

4. Results and discussions

4.1. Performance of trays and corrugated trays solar stills with and without internal mirrors

The spaces between the trays have been used to fix the internal mirrors to reduce the rate of heat loss from the distiller walls and reflect solar radiation onto the trays. The glass and water temperatures of the FTSS and CTSS with internal reflectors as well as the solar radiation intensity and ambient air temperatures were measured, as presented in Fig. 5.

For the trays solar still, without the internal reflectors, the average water temperature of the trays distiller was less than that of the conventional distiller by about 0 – 1.5°C. In addition, the glass temperature for FTSS and CTSS were found to be higher than that of the conventional still by about 0 – 1.5°C. This is due to increase in the rates evaporation and condensation of the water vapor in the trays still compared to the conventional counterpart. The maximum hourly solar radiation intensity of 950 W/m^2 was obtained at noon (12:00). Furthermore, the maximum glass/water temperatures at 13:00 for the CTSS, FTSS without reflectors and the CSS were found to be 42.5°C/60.5°C, 42°C/60°C and 41°C/61.5°C, respectively, as shown in Fig. 3. Also, the accumulated distillate water obtained from the CTSS, FTSS without reflectors and the CSS were 3350, 2900 and 2000 mL/m^2 a day, respectively, as shown in Fig. 4. Additionally, the productivity enhancement by the FTSS was found to be 45% more than that of the CSS. This achievement was largely due to the 73% increase in evaporation area of the trays still

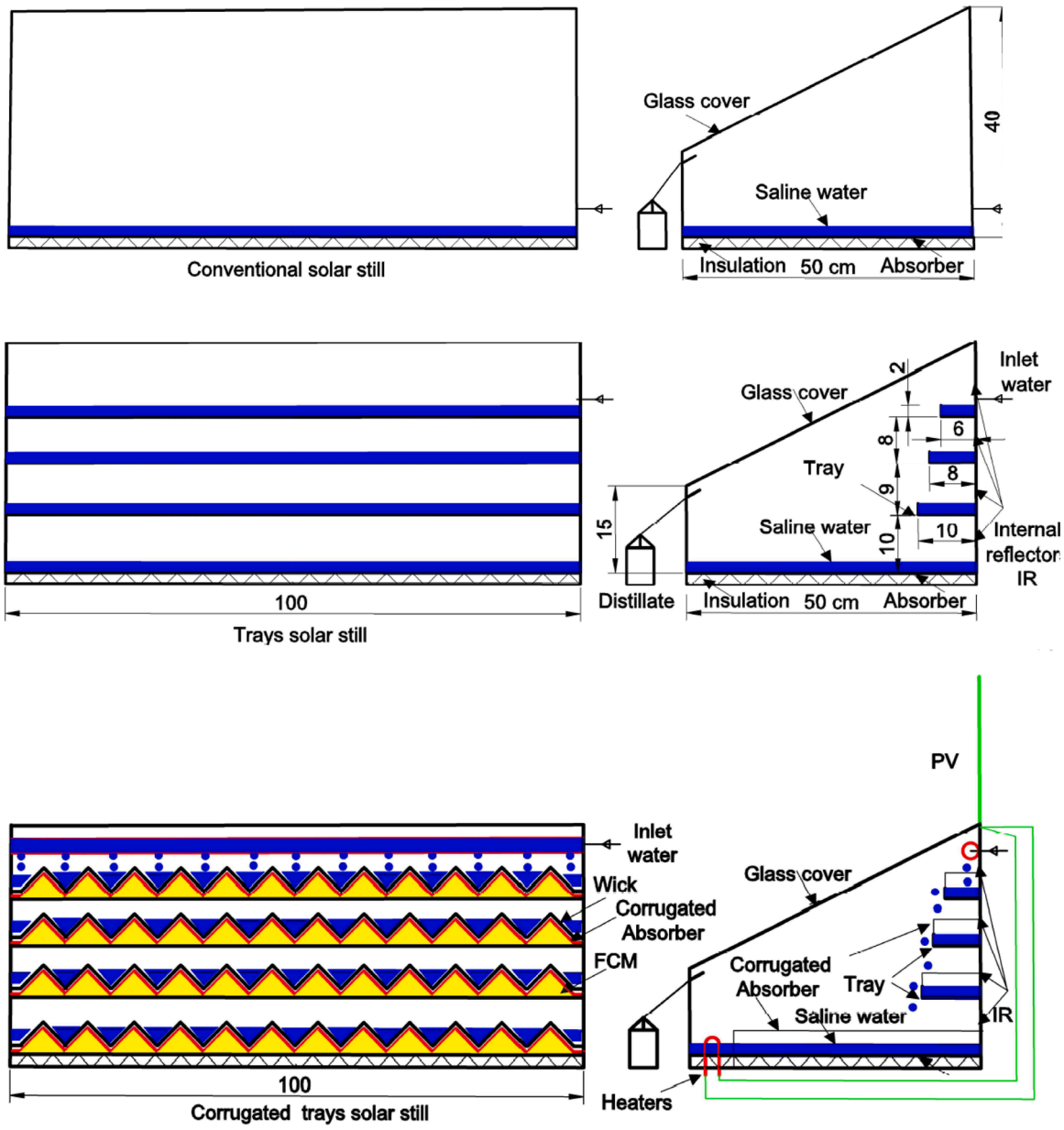

Fig. 2. Schematic of tested solar stills.

Table 1
Thermo-physical properties of paraffin wax and paraffin wax with nanoparticles.

Property	Paraffin wax	Paraffin wax with CuO nanoparticles
Density	876 kg/m^3	941 kg/m^3
Melting point	54 °C	53 °C
Latent heat of fusion	190 kJ/kg°C	187 kJ/kg°C
Specific heat	2.1 kJ/kg°C	2.05 kJ/kg°C
Thermal conductivity	0.21W/m°C	0.28 W/m°C

Table 2
CuO nanoparticles properties.

Chemical composition	Size, nm	Density, kg/m^3	Specific heat, J/mol K	Thermal conductivity, W/m K
CuO	10-14	6320	42.36	76.5

Table 3
Thermal conductivity of PCM with nanoparticles at different nanoparticles concentration.

Concentration of CuO by wt, %	0	0.5	1.5	2.5	3.5	4.5
Thermal conductivity, W/m°C	0.21	0.233	0.25	0.28	0.284	0.286

Table 4
Instruments uncertainties, errors and measuring range.

Instrument	Accuracy	Range	Error, %
Wind Anemometer	± 0.1 m/s	0.4 – 30 m/s	3
Flask	±5 mL	0 – 2000 mL	2
Solarimeter	± 1 W/m^2	0 – 5000 W/m^2	1.5
Thermocouples	± 0.1°C	0 – 100°C	1.3
Multimeter	± 1 V	0 – 1000 V	0.5
	± 0.1 A	0-10 A	5

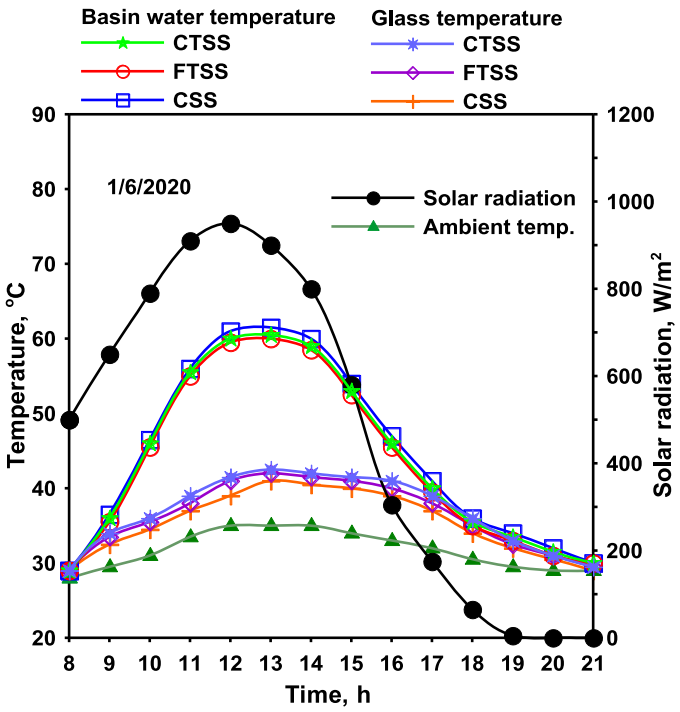

Fig. 3. Environmental conditions and temperatures of water and glass of tested SS.

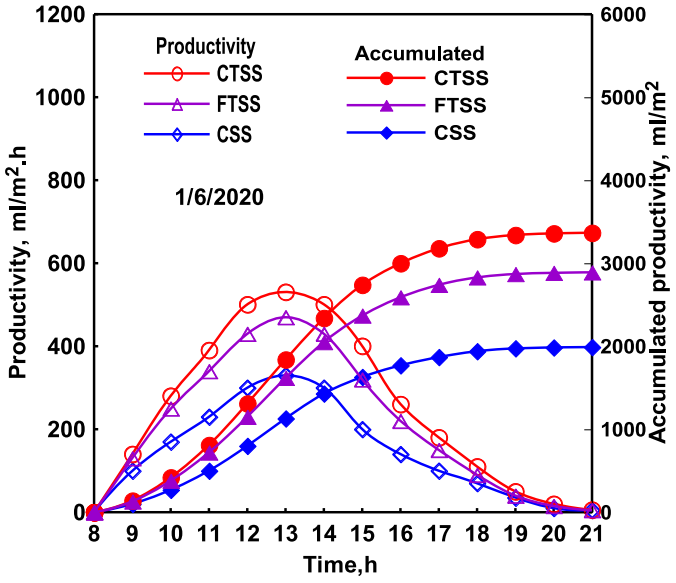

Fig. 4. The hourly variations of productivity of tested solar stills.

compared to the conventional counterpart. In addition, the absorber surface area of the CTSS was about 150% more than the CSS. The productivity enhancement by the CTSS was found to be 67.5% more than that of the CSS.

The variations of the atmospheric air temperature, solar radiation, and basin water temperatures of three tested solar stills (trays stills with internal reflectors, IR) at the same water depth (2 cm) are presented in Fig. 5. It can be seen that all the temperature profiles increase with time until they reached a maximum value in afternoon and then decreases afterwards. This follows the solar radiation intensity variation pattern with increase in the radiation before noon and its decrease in the afternoon with the peak at noon. Also, Fig. 5 showed that the maximum

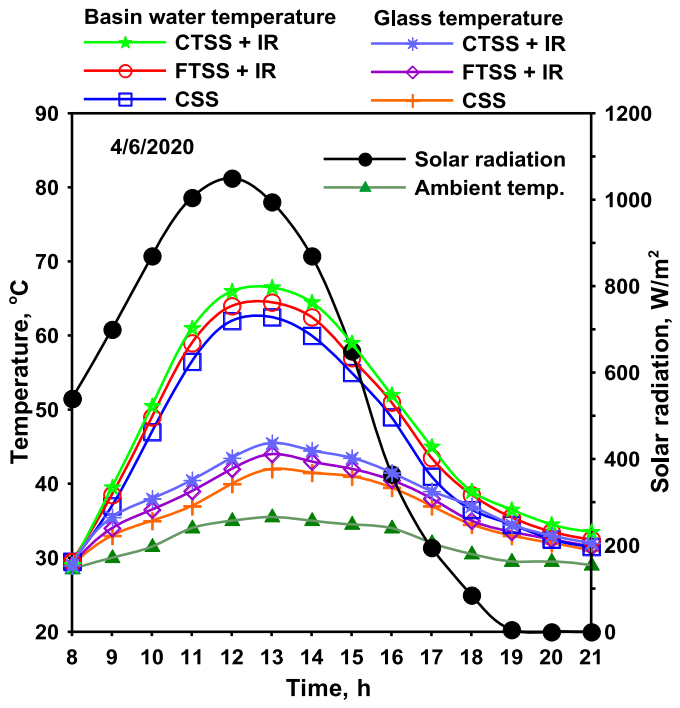

Fig. 5. Environmental conditions and temperatures of water and glass of tested SS with IR.

temperatures was obtained at 1:00pm (13:00) while the maximum solar radiation was at noon (12:00).

Comparisons between the temperature of basin water from (from 8 a.m. to 9 p.m.) for the three systems were shown in Fig. 5. It was found that the average water temperature of basin of the corrugated trays solar still (CTSS) was higher than that of trays (FTSS) and the conventional still (CSS). Meanwhile, the use of internal reflectors (IR) increases the temperature of the basin water in the trays solar still more than the CSS by about 0 – 2 °C. While the basin water temperature of the CTSS was greater than that of CSS by about 0 – 4 °C.

The CSS glass temperature shows lower values than that for FTSS and CTSS with reflectors by 0 – 2 °C and 0 – 3.5 °C, respectively. The reason for the high glass temperature for FTSS and CTSS was the rapid evaporation rate. This was attributed to adding mirrors and the high water temperature. The maximum solar irradiance of 1050 W/m^2 was also obtained at noon (12:00). Also, the highest temperatures of glass/water were 45.5 °C/66.5 °C, 44 ℃/64.5 °C and 42 °C/62.5 °C for CTSS, FTSS and CSS at 13:00, respectively.

Fig. 5 Also showed that the temperatures of glass and basin water of CTSS with wick were more than that of FTSS and CSS. This may be due to the following: (1) the wick material has higher storage material properties than that of the water only, (2) in the wick, the feed water flows very slowly through a porous to upward, radiation absorbing pad (the wick) and (3) the wick capillarity helped in exposing small amount of water to solar radiation in the evaporation surface without need to heat bulk water as in the CSS case. For these reasons, the freshwater production rate from the CTSS is more than that of FTSS and CSS as the ability of evaporation and condensation rates is also higher in the CTSS.

The hourly water temperature variations for basin liner of the three trays (upper, intermediate and lower), as well as the average temperature of water for the FTSS with reflectors are presented in Table 5. The upper tray was found to have higher water temperatures than the lower and intermediate trays and the basin liner. In addition, the basin liner water temperature was found to be the minimum. Furthermore, the following relation was used to calculate the average water temperature based on the water mass (m) specific heat capacity (C_P), and element temperature (T).

Table 5
Water temperature of the trays and basin of FTSS with reflectors.

hour	Trays temperature, ℃			Basin, °C	Average, °C
	Upper	intermediate	lower		
8	29.5	29.3	29	28	29
9	44	42.5	41	38	39
10	54	52.5	50	47	48.5
11	65.5	63.5	61	57	58.5
12	72	70.8	68	63	64
13	73	72	68.7	64	64.5
14	70.6	68.5	65	61	63
15	66	64	61	57	57
16	59	57.5	54	50.5	52
17	51	49.5	47	44	44
18	44	43.5	42	40	40
19	38	37	36	35	35.5
20	34	33.5	33	32	32.5
21	31	30.8	30.5	30	30.5

$$m_{total} \times Cp_{paverage} \times T_{average} = (m \times Cp \times T)_{basin} + (m \times Cp \times T)_{lower\ tray} + (m \times Cp \times T)_{intermediate\ tray} + (m \times Cp \times T)_{upper\ tray}$$

Comparisons between the instantaneous variations of hourly distillate and accumulated water production from 8 a.m. to 9 p.m. for the three tested stills are shown in Fig. 6. It was found that the amount of accumulated distillate water for the CTSS was higher than that of FTSS and CSS. It was also found that the CTSS and FTSS with reflectors produced more hourly distillate than the conventional distiller. This was largely due to the larger evaporative surface area resulting in higher evaporation rates in the CTSS and FTSS as compared to the CSS. In addition, they have a higher water temperature. The water evaporation surface areas for conventional and trays solar stills were 0.5m^2 and 0.865m^2, respectively. The evaporation surface area of trays solar still is divided into 0.5, 0.0696, 0.1152 and 0.18 m^2 for the basin liner, upper tray, intermediate tray and lower tray, respectively. Hence, the evaporative surface area of the trays distiller was about 73% greater than the CSS. Besides, the internal mirrors reduce the heat losses from the back wall of the still distiller by reflecting the solar radiation onto the trays water. On the other hand, the evaporative surface area of the corrugated trays still (1.25 m^2) was subdivided into 0.78, 0.099, 0.159, and 0.215 m^2 for the basin liner, upper tray, intermediate tray and lower tray, respectively. Similarly, the absorber surface area of the CTSS was about 150% more than the conventional distiller. Also, the internal mirrors reduce the heat losses from the back wall of the still distiller by reflecting the solar radiation onto the trays water.

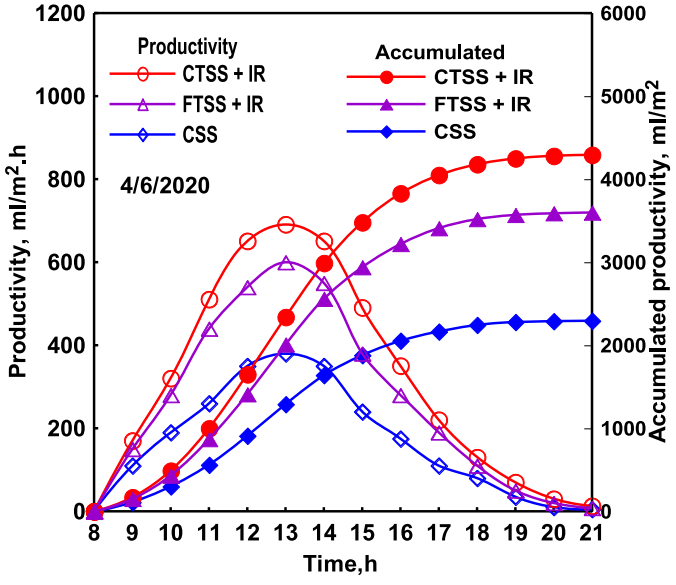

Fig. 6. The hourly variations of productivity of tested solar stills with internal reflectors.

Fig. 6 illustrates that the CSS, FTSS and CTSS have a maximum hourly production of 380, 600 and 680 mL/m^2 at 1pm, respectively. Also, the total freshwater productivity of both distillers are shown in Fig. 6. It can be seen that the total freshwater productivity of the CSS, FTSS and CTSS were 2300, 3600 and 4300 mL/m^2, respectively with respective percentages improvement of 57% and 87% for the FTSS and CTSS compared to the CSS.

4.2. Effect of raising the water temperature of the CTSS using heaters and PV panel

To investigate the influence of heating the basin water of CTSS using three electric heaters with a power of 30 W each. The heaters were immersed into the basin water of the CTSS to heat the water of the still. Also, these heaters were run using a PV system with a power of 120 W.

Fig. 7 shows the distribution of solar radiation, PV power, temperatures of the CSS and CTSS with electric heaters. It can be concluded from Fig. 7 that the behavior of the PV energy is the same as that of the solar irradiance. Where it increases with increasing the solar radiation and decreases with the decline of solar intensity. Comparing the results obtained from Fig. 5 and Fig. 7, incorporating the electric heaters into the basin water of the CTSS led to raise the basin water temperature, and it was always higher than that of the CSS. the readings revealed that, the difference between the water temperatures of the CSS and CTSS with heaters was about 18°C at 13:00, as illustrated in Fig. 7. The maximum water temperature was obtained at 13:00, where it was 82°C and 64°C for the CTSS with heaters and CSS, respectively. Moreover, the raised water temperature of the CTSS with heaters led to increase the vapor content generation compared to the first case of CTSS without heaters. This increased the glass temperature of CTSS over that of the CSS by 0 – 5°C. The maximum glass temperature was obtained at 13:00, where it was 43°C and 48°C for the CSS and CTSS with heaters, respectively.

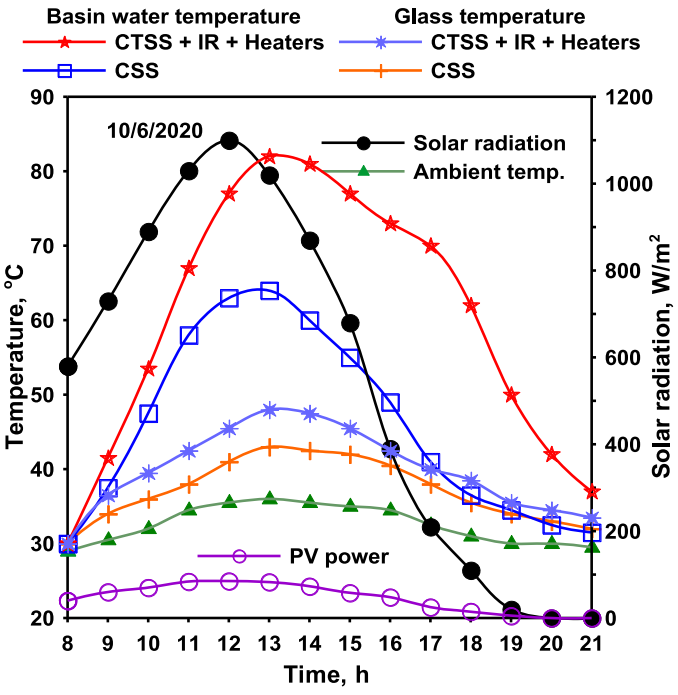

Fig. 7. Distribution of solar radiation, PV power and temperatures of SS with heaters and PV.

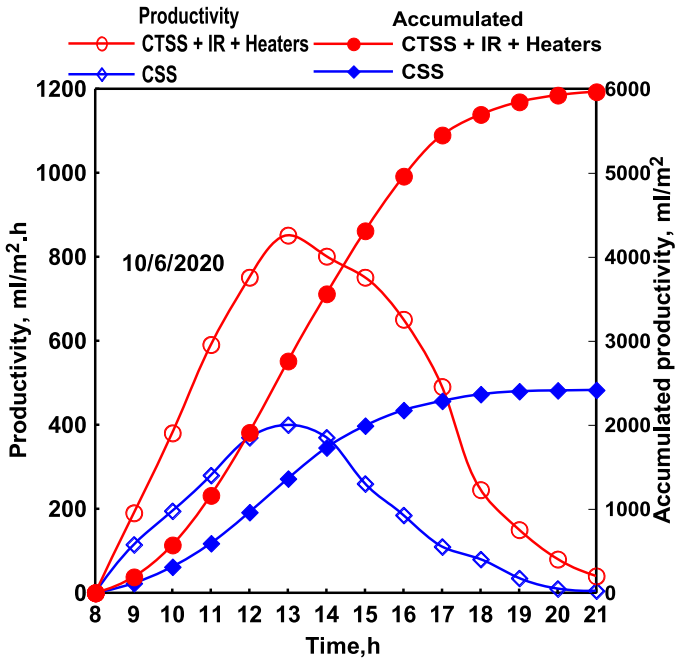

Fig. 8. Hourly and total productivity of CSS and CTSS with electric heaters.

The variations of the hourly and total freshwater productivity of the CSS and CTSS with electric heaters was illustrated in Fig. 8. It can be observed from the figure that the hourly and total productivities of the CTSS with electric heaters were always greater than that of the CSS. This can be reasoned by the previous two reasons explained in section 4.1 plus the existence of the electric heaters that augmented the vapor generation inside the solar still by raising the water temperature. Furthermore, the hourly productivity was maximum at 13:00, where the maximum productivities of the CTSS with heaters and CSS were 850 and 400 mL/m^2.hr, respectively.

As well Fig. 8 illustrates that, the total productivity of the CTSS with electric heaters was more than that of the CSS. It was concluded that the total distillates of the CTSS with heaters and CSS were 6000 and 2400 mL/m^2 a day, respectively. So, the productivity was enhanced by 150%. So, the This augmentation of productivity can be referred to the superior evaporation of the CTSS with heaters over that of the conventional still. Therefore, the rate of increase resulting from the presence of electric heaters is 63%.

$$\eta_d(\text{daily thermal efficiency}) = \frac{\text{The daily yield} \times \text{Vaporization latent heat}}{\text{The daily solar radiation incidence on condensing surface area}}$$

4.3. Performance of CTSS when using PCM with CuO nanoparticles

From the previous section it can be found that the CTSS shows better performance when compared with CSS and FTSS. For further improvement in CTSS performance a PCM and CuO nanoparticles have been used together. Fig. 9 shows the hourly water temperature profiles of the CTSS with PCM and CuO. It can be seen that the temperatures have initially been increased and reached the maximum point at 13:00, and started to decline in response to the decrease in solar radiation intensity. At the beginning of the experiment, the PCM absorbed thermal energy from the distiller absorber plate (Heating process). During the heating process, the PCM stores the absorbed energy as sensible heat from the absorber plate. The PCM charging process begins from early morning with obvious rise in the temperature. The PCM and water temperatures have been increased gradually with the increase in solar radiation intensity and ambient temperature reaching maximum values at 13:00. Besides, the discharging process started when the intensity of the solar irradiance began to decrease after 13:00, as illustrated in Fig. 9. This resulted in the drop of the PCM temperature due to the heat released from the PCM to the water. This decrease in the temperature of the PCM continued until it reached the ambient condition at 9 pm.

Fig. 10 shows the hourly and accumulated productivities of the CSS and CTSS with PCM and CuO nanoparticles. In the early hour from 8:00 to 9:00, the productivities of both solar stills (CSS and CTSS) are so close. Then, after 9:00, although it is the time of charging period of CTSS, the productivity of the CTSS is observed to be increased remarkably as compared to that of the CSS. Because the water temperature of the CTSS is still higher than CSS, in addition to the CTSS has large area and the internal reflectors. This charging time extended up to 13:00 when the maximum hourly freshwater was observed from both the solar distillers. After 13:00, as the intensity of solar radiation decreases, there was decrease in the hourly fresh water productivity of the CSS. Despite the decrease in solar intensity after 13:00, the corrugated solar still yielded more productive than the CSS during the same period, as shown in Fig. 10. This improvement was attributed to the absorbed heat energy by the PCM which was released during the discharging time. In addition, it is noticed from the figure that decrease rate of the productivity of CSS (from 13:00 to 18:00 pm) is fast compared to that of the CTSS, which is due to released heat from the PCM during the discharging time. Also Fig. 10 revealed that, the amount of accumulated freshwater from the CSS and CTSS were 2500 and 5550 mL/m^2 per day, respectively. The productivity enhancement from CTSS was 122% more than the conventional CSS when using PCM with CuO nanoparticles. Consequently, using CuO nanoparticles mixed with paraffin wax only resulted in an increase in the fresh water productivity of the CTSS by 35% over the CTSS without PCM. On the other hand, the results show that, the CTSS yielded an improvement in the daily productivity by 180% more than the CSS when using IR, heaters and PCM with CuO nanoparticles. Where the daily fresh water production is 2500 and 7000 mL/m^2 for CSS and CTSS, respectively.

4.4. Efficiency of solar distillers

The daily thermal efficiency is a key factor to obtain the performance of the solar still. this factor is determined as [47];

$$\eta_d = \frac{\sum \dot{m} \times h_{fg}}{\sum A \times I(t)} \quad (7)$$

As well, h_{fg} is computed as following [54];

$$h_{fg} = 3.1625 \times 10^6 + \left[1 - \left(7.616 \times 10^{-4} \times T_w\right)\right] \text{ for } T_w > 70^\circ C \quad (8)$$

$$h_{fg} = 2.4935 \times 10^6 \left[1 - \left(9.4779 \times 10^{-4} \times T_w\right) + \left(1.3132 \times 10^{-7} \times T_w^2\right) - \left(4.7974 \times 10^{-9} \times T_w^3\right)\right] \text{ for } T_w < 70^\circ C \quad (9)$$

where T_w is the water temperature. Regarding the above equations, the daily thermal efficiency of the CSS and CTSS under various operating conditions is plotted in Fig. 11. It is obtained from Fig. 11 that the

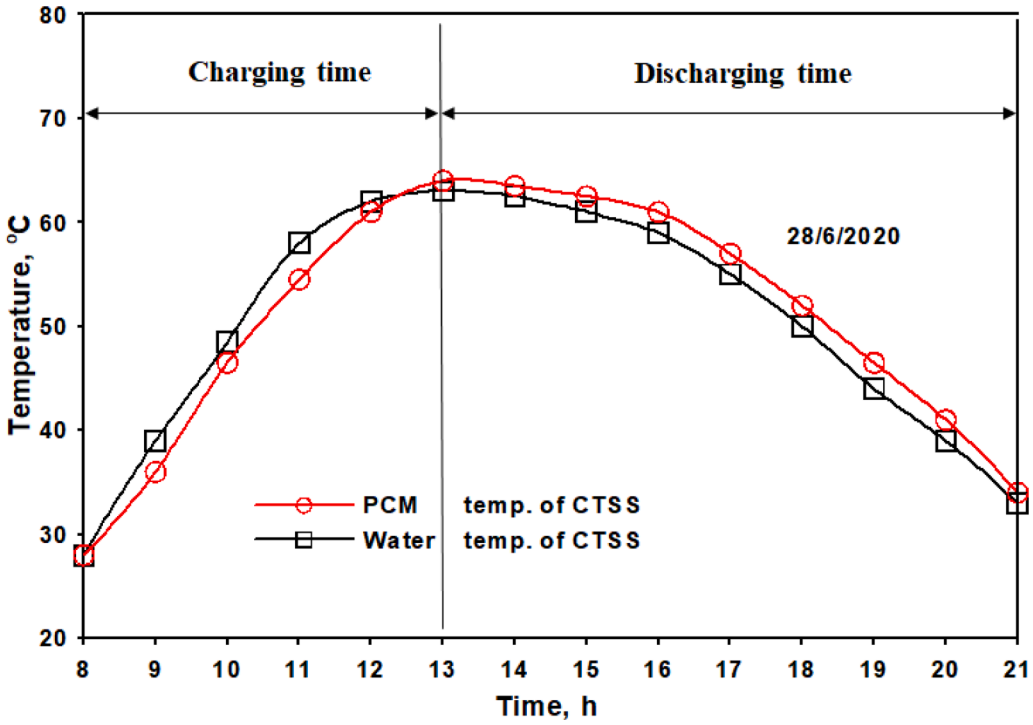

Fig. 9. The temperatures of PCM and water of CTSS.

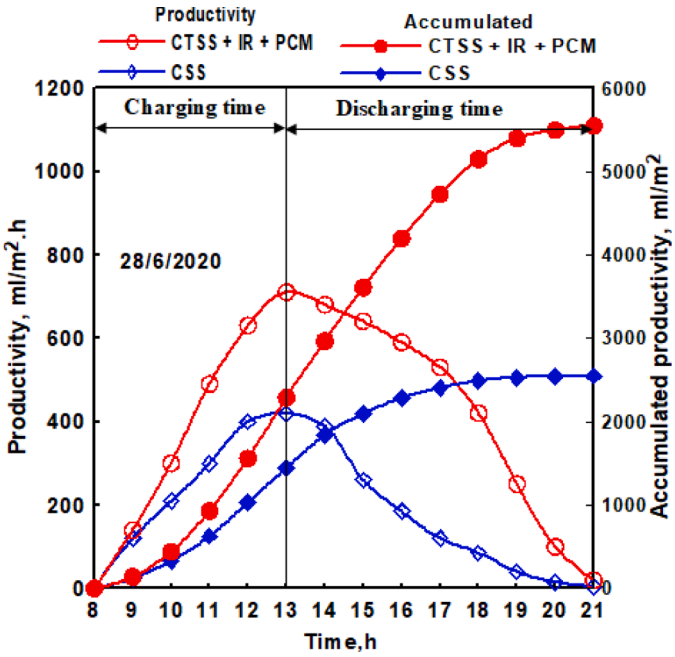

Fig. 10. Hourly and accumulate productivity of CSS and CTSS with PCM and CuO nanoparticles.

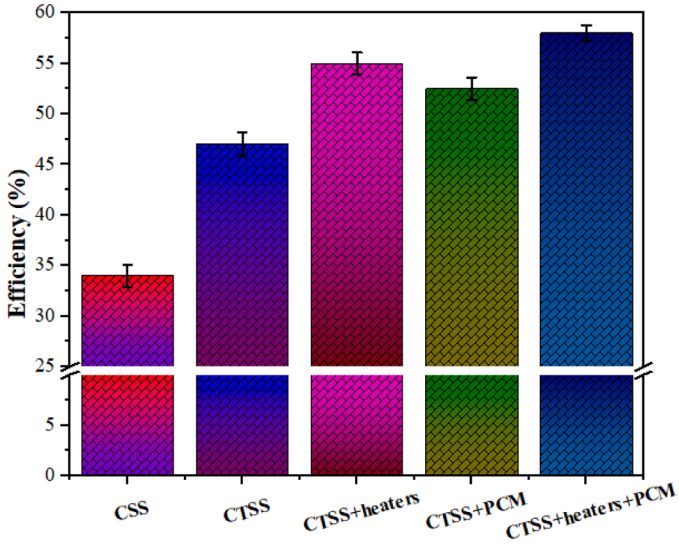

Fig. 11. Efficiency of CSS and CTSS under different investigated conditions.

thermal efficiency of the CTSS was 47 % and 54 % when with heaters, respectively. In addition, using PCM with nanoparticles enhanced the thermal efficiency of the CTSS to 52.3 % and 57 % when using heaters and PCM with nanoparticles, respectively. Finally, as found from Fig. 11, the average daily thermal efficiency of the CSS was around 34 %.

5. Cost analysis

The cost calculations for the studied solar stills varies with the still type and its components, Table 6. The cost per liter of fresh water produced from CSS, CTSS, CTSS with electric heaters and CTSS with nano-enhanced PCM has been estimated using the following equations, (Bait [55], Essa et al. [56]),

The capital recovery factor (CRF) has been estimated as following:

$$CRF = \frac{i\,(1+i)^n}{(1+i)^n - 1} \tag{10}$$

Wherever, i and n are the interest rate and SS life time (years), respectively.

The annual fixed cost (FAC) is:

$$FAC = P\left(\frac{i\,(1+i)^n}{(1+i)^n - 1}\right) \tag{11}$$

Table 6
Fabrication cost for 1 m^2 of CSS and CTSS.

Unit	CSS ($)	CTSS	CTSS+heaters	CTSS+PCM	CTSS+heaters+ PCM
Galvanized steel	30	30	30	30	30
CTSS absorber	-	15	15	15	15
Glass cover	10	10	10	10	10
Ducts and support legs	25	25	25	25	25
Production	20	40	40	40	40
Black paint	5	7	7	7	7
Insulation	7	7	7	7	7
Mirrors	-	5	5	5	5
Electric heaters	-	-	10	-	10
PV	-	-	55	-	55
PCM	-	-	-	11	11
Nanoparticles	-	-	-	30	30
Capital cost (P)	97	139	204	180	245

Where, P is the capital cost of SS ($)
The annual salvage cost (ASC) is:

$$ASC = \mathrm{S}\left(\frac{i}{(1+i)^n - 1}\right) \tag{12}$$

Where S is taken as:

$$S = 0.2\ P \tag{13}$$

The operating and maintenance annual cost (AMC)

$$AMC = 0.15\left(P\left(\frac{i\ (1+i)^n}{(1+i)^n - 1}\right)\right) \tag{14}$$

The total annual cost (TC)

$$TC = \mathrm{FAC} + \mathrm{AMC} - \mathrm{ASC} \tag{15}$$

The price of fresh water per liter (PPL) in $ per is

$$PPL = TC/Y \tag{16}$$

Where, Y is the average annual fresh water yield.
The next assumptions have been considered: the yearly working days have been assumed to be 340 days, 10 years is SS life time, the rate of interest is 15%. Furthermore, the average daily production, the capital cost and cost per liter of produced water are tabulated in Table 7.

6. Conclusions

In the current work, getting an increase of absorber surface area of trays solar still was targeted for better evaporation. As a result, the trays solar stills with flat and corrugated absorber configurations have been investigated. According to the explained findings of the tested solar stills, the following conclusions can be drawn;

1- The proposed design of the corrugated trays solar still led to enlarge the evaporative surface area of the CTSS by 150% compared to that of the CSS.
2- Without heaters, the total distillates of the CSS, FTSS and CTSS were 2300, 3600 and 4300 mL/m^2 respectively, with percentage improvements of 57% and 87% for the FTSS and CTSS compared to the CSS.
3- Using the electric heaters, the total distillates of the CTSS and CSS were 6000 and 2400 mL/m^2 a day, respectively. So, the productivity was enhanced by 150%.
4- When using PCM with CuO nanoparticles with CTSS, the total daily production of the CSS and CTSS are 2500 and 5550 mL/m^2 a day, respectively. So, the productivity was enhanced by 122% over the CSS.
5- The total water productivity of the CTSS was improved by 180% when using PCM with CuO nanoparticles and electrical heaters over that of the CSS.

Table 7
Average daily production, capital cost and cost per liter of produced water for tested SS.

	CSS ($)	CTSS	CTSS+ heaters	CTSS+ PCM	CTSS+ heaters+ PCM
Capital cost (P), $	97	139	204	180	245
Average daily production, L/m^2	2.2	4.1	5.5	4.9	6.2
Cost per liter, $	0.028	0.022	0.0239	0.0236	0.025

6- The thermal efficiency for CSS and CTSS with PCM- CuO nanoparticles and electrical heaters has been calculated to be 34% and 57%, respectively.
7- The estimated costs of produced fresh water per liter from CSS and CTSS with PCM-CuO nanoparticles and electrical heaters have been calculated to be 0.028 and 0.025 $, respectively.

Further studies are proposed as follows:

1 Using a different shape for the trays distiller absorber.
2 Eexternal reflectors.
3 Conduct a theoretical study of the optimum dimensions of the trays.
4 Conduct a theoretical study of the optimum dimensions of the corrugated absorber's.

Declaration of Competing Interest

There is no conflict of interest.

Acknowledgments

This project was supported by the Deanship of Scientific Research at Prince Sattam Bin Abdulaziz University under the research project number 2020/01/17122.

References

[1] H. Chang, et al., Highly efficient reverse osmosis concentrate remediation by microalgae for biolipid production assisted with electrooxidation, Water Res. 174 (2020), 115642.
[2] A.S. Abdullah, Z.M. Omara, M.A. Bek, F.A. Essa, An augmented productivity of solar distillers integrated to HDH unit: Experimental implementation, Appl. Therm. Eng. 167 (2020), 114723.
[3] A.S. Abdullah, F.A. Essa, Z.M. Omara, M.A. Bek, Performance evaluation of a humidification–dehumidification unit integrated with wick solar stills under different operating conditions, Desalination 441 (2018) 52–61.
[4] F.A. Essa, A.S. Abdullah, Z.M. Omara, A.E. Kabeel, Wael M El-Maghlany, On the Different Packing Materials of Humidification–Dehumidification Thermal Desalination Techniques–A Review, Cleaner Production, 2020, 123468.
[5] H. Wu, et al., Effect of droplets on water vapor compression performance, Desalination 464 (2019) 33–47.

[6] H. Lv, et al., Numerical simulation and optimization of the flash chamber for multi-stage flash seawater desalination, Desalination 465 (2019) 69–78.
[7] M.A. Darwish, F. Al-Juwayhel, H.K. Abdulraheim, Multi-effect boiling systems from an energy viewpoint, Desalination 194 (1) (2006) 22–39.
[8] Z.M. Omara, A.E Kabeel, Performance of different sandy beds solar still, Int. J. Green Energy 11 (2014) 240–254.
[9] F. Essa, M. Abd Elaziz, A.H. Elsheikh, An enhanced productivity prediction model of active solar still using artificial neural network and Harris Hawks optimizer, Appl. Therm. Eng. 170 (2020), 115020.
[10] A.E. Kabeel, A. Khalil, Z.M. Omara, M.M. Younes, Theoretical and experimental parametric study of modified stepped solar still, Desalination 289 (2012) 12–20.
[11] J. Ward, A plastic solar water purifier with high output, Sol. Energy 75 (2003) 433–437.
[12] Z.M. Omara, Mohamed A. Eltawil, Hybrid of solar dish concentrator, new boiler and simple solar collector for brackish water desalination, Desalination 326 (2013) 62–68.
[13] Mohamed A. Eltawil, Z.M. Omara, Enhancing the solar still performance using solar photovoltaic, flat plate collector and hot air, Desalination 349 (2014) 1–9.
[14] A.R.A. Elbar, H. Hassan, Enhancement of hybrid solar desalination system composed of solar panel and solar still by using porous material and saline water preheating, Sol. Energy 204 (2020) 382–394.
[15] Z.M. Omara, A.E. Kabeel, M.M. Younes, Enhancing the stepped solar still performance using internal reflectors, Desalination 314 (2013) 67–72.
[16] K.M. Bataineh, M.A. Abbas, Performance analysis of solar still integrated with internal reflectors and fins, Sol. Energy 205 (2020) 22–36.
[17] H. Hassan, M.S. Yousef, M. Fathy, M.S. Ahmed, Assessment of parabolic trough solar collector assisted solar still at various saline water mediums via energy, exergy, exergoeconomic, and enviroeconomic approaches, Renew. Energ. (2020).
[18] HosseinAmiri.Mohammad Aminy, Marzieh Lotfi, Behzad Jafar beglo. Energy and exergy analysis of a new solar still composed of parabolic trough collector with built-in solar still, Renew. Energ. (2021) 465–479.
[19] O. Bait, Exergy, environ–economic and economic analyses of a tubular solar water heater assisted solar still, J. Cleaner Prod. 212 (2019) 630–646.
[20] Z.M. Omara, A.E. Kabeel, A.S. Abdullah, F.A. Essa, Experimental investigation of corrugated absorber solar still with wick and reflectors, Desalination 381 (2016) 111–116.
[21] Z.M. Omara, A.E. Kabeel, F.A. Essa, Effect of using nanofluids and providing vacuum on the yield of corrugated wick solar still, Energy Convers. Manage. 103 (2015) 965–972.
[22] Z.M. Omara, Mofreh H. Hamed, A.E. Kabeel, “Performance of finned and corrugated absorbers solar stills under Egyptian conditions”, Desalination, 277 (2011) 281-287.
[23] Z.M. Omara, M.A. Eltawil, E.A. ElNashar, A new hybrid desalination system using wicks/solar still and evacuated solar water heater, Desalination 325 (2013) 56–64.
[24] V. Velmurugan, S. Pandiarajan, P. Guruparan, L.H. Subramanian, C.D. Prabaharan, K. Srithar, Integrated performance of stepped and single basin solar stills with mini solar pond, Desalination 249 (2009) 902–909.
[25] Z.M. Omara, A.E. Kabeel, M.M. Younes, Enhancing the stepped solar still performance using internal and external reflectors, Energy Convers. Manage. 78 (2014) 876–881.
[26] F.A. Essa, Z.M. Omara, A.S. Abdullah, S. Shanmugan, Hitesh Panchal, A.E. Kabeel, Ravishankar Sathyamurthy, Wissam H Alawee, A Muthu Manokar, Ammar H Elsheikh., Wall-suspended trays inside stepped distiller with Al2O3/paraffin wax mixture and vapor suction: Experimental implementation, Energy Storage 32 (2020), 102008.
[27] Z.S. Abdel-Rehim, A. Lasheen, Improving the performance of solar desalination systems, Renew. Energ. 30 (13) (2005) 1955–1971.
[28] A.E. Kabeel, M.H. Hamed, Z.M. Omara, Augmentation of the basin type solar still using photovoltaic powered turbulence system, Desalin. Water Treat. 48 (2012) 182–190.
[29] Z.M. Omara, A.S. Abdullah, T. Dakrory, Improving the productivity of solar still by using water fan and wind turbine, Sol. Energy 147 (2017) 181–188.
[30] A. Abdullah, A. Alarjani, M.A. Al-sood, Z. Omara, A. Kabeel, F. Essa, Rotating-wick solar still with mended evaporation technics: Experimental approach, Alexandria Eng. J. 58 (2019) 1449–1459.
[31] AS Abdullah, ZM Omara, FA Essa, A Alarjani, Ibrahim B Mansir, M. Amro, Enhancing the solar still performance using reflectors and sliding-wick belt, Sol. Energy 214 (2021) 268–279.
[32] F.A. Essa, A.S. Abdullah, Z.M. Omara, Improving the performance of tubular solar still using rotating drum – Experimental and theoretical investigation, Process Saf. Environ. Prot. 148 (2021) 579–589.
[33] F.A. Essa, A.S. Abdullah, Z.M. Omara, Rotating discs solar still: New mechanism of desalination, J. Cleaner Prod. 275 (2020), 123200.
[34] A. Abdullah, F. Essa, Z. Omara, Y. Rashid, L. Hadj-Taieb, G. Abdelaziz, et al., Rotating-drum solar still with enhanced evaporation and condensation techniques: Comprehensive study, Energy Convers. Manage 199 (2019), 112024.
[35] AS Abdullah, ZM Omara, A Alarjani, FA Essa, Experimental investigation of a new design of drum solar still with reflectors under different conditions, Case Studies in Thermal Eng. 24 (2021), 100850.
[36] WH Alawee, FA Essa, SA Mohammed, HA Dhahad, AS Abdullah, ZM Omara Improving the performance of pyramid solar still using rotating four cylinders and three electric heaters, Process Saf. Environ. Prot. 148 (2021) 950–958.
[37] A.E. Kabeel, Z.M. Omara, F.A. Essa, Enhancement of modified solar still integrated with external condenser using nanofluids: An experimental approach, Int. J. Energy Convers. Manage. 78 (2014) 493–498.
[38] T. Arunkumar, Effect of nano-coated CuO absorbers with PVA sponges in solar water desalting system, Appl. Therm. Eng. 148 (2019) 1416–1424.
[39] M. Al-Shammiri, Evaporation rate as a function of water salinity, Desalination 150 (2) (2002) 189–203.
[40] A.A Badran, Assaf K.S. Kayed, F.A. Ghaith, d M.I. Hammash, Simulation and experimental study for an inverted trickle solar still, Desalination 164 (2004) 77–85.
[41] B.A. Akash, M.S. Mohsen, W. Nayfeh, Experimental study of the basin type solar still under local climate conditions, Energy Convers. Manag. 41 (9) (2000) 883–890.
[42] R. Kalbasi, M.N. Esfahani, Multi-effect passive desalination system, an experimental approach, World Appl. Sci. J. 10 (10) (2010) 1264–1271.
[43] Asiful Hoque, Ashif Hasan Abir, Kironmoy Paul Shourov, Solar still for saline water desalination for low-income coastal areas, Appl. Water Sci. 9 (2019) 104.
[44] K. Ranjan, S. Kaushik, N. Panwar, Energy and exergy analysis of passive solar distillation systems, Int. J. Low-Carbon Technol. 11 (2016) 211–221.
[45] A.S. Abdullah, M. Younes, Z.M. Omara, F.A. Essa, New design of trays solar still with enhanced evaporation methods–Comprehensive study, Sol. Energy 203 (2020) 164–174.
[46] F.A. Essa, A.S. Abdullah, Z.M. Omara, AE Kabeel, Y Gamiel, Experimental study on the performance of trays solar still with cracks and reflectors, Appl. Therm. Eng. 188 (2021), 116652.
[47] A.S. Abdullah, F.A. Essa, H.B. Bacha, Z.M. Omara, Improving the trays solar still performance using reflectors and phase change material with nanoparticles, J. Energy Storage 31 (2020), 101744.
[48] A.E. Kabeel, K. Harby, M. Abdelgaied, A. Eisa, Augmentation of a developed tubular solar still productivity using hybrid storage medium and CPC: An experimental approach, J. Energy Storage 28 (2020), 101203.
[49] V.S. Vigneswaran, G. Kumaresan, B.V. Dinakar, K.K. Kamal, R. Velraj, Augmenting the productivity of solar still using multiple PCMs as heat energy storage, Energy Storage 26 (2019), 101019.
[50] A.E. Kabeel, M. Abdelgaied, Improving the performance of solar still by using PCM as a thermal storage medium under Egyptian conditions, Desalination 383 (2016) 22–28.
[51] V.P. Katekar, S.S. Deshmukh, A review of the use of phase change materials on performance of solar stills, Energy Storage 30 (2020), 101398.
[52] L. Sahota, G. Tiwari, Effect of nanofluids on the performance of passive double slope solar still: a comparative study using characteristic curve, Desalination 388 (2016) 9–21.
[53] J. Holman, Experimental Methods for Engineers, McGraw-Hill Companies, New York, 2012. Eighth ed.
[54] G.N. Tiwari, L. Sahota, Advanced Solar-Distillation Systems: Basic Principles, Thermal Modeling, and Its Application, Springer, 2017.
[55] O. Bait, Exergy, environ–economic and economic analyses of a tubular solar water heater assisted solar still, J. Cleaner Prod. 212 (2019) 630–646.
[56] F.A. Essa, W.H. Alawee, S.A. Mohammed, A.S. Abdullah, Z.M. Omara, Enhancement of pyramid solar distiller performance using reflectors, cooling cycle, and dangled cords of wicks, Desalination 506 (2021), 115019.